

EAGLE: EXPLORING THE DESIGN SPACE FOR MULTI-MODAL LLMs WITH MIXTURE OF ENCODERS

Min Shi^{2*}, Fuxiao Liu^{3*}, Shihao Wang⁴, Shijia Liao¹, Subhashree Radhakrishnan¹,
Yilin Zhao⁵, De-An Huang¹, Hongxu Yin¹, Karan Sapra¹, Yaser Yacoob³, Humphrey Shi²,
Bryan Catanzaro¹, Andrew Tao¹, Jan Kautz¹, Zhiding Yu^{1†}, Guilin Liu^{1†}

¹NVIDIA ²Georgia Tech ³UMD ⁴HKPU ⁵NYU

<https://github.com/NVlabs/Eagle>

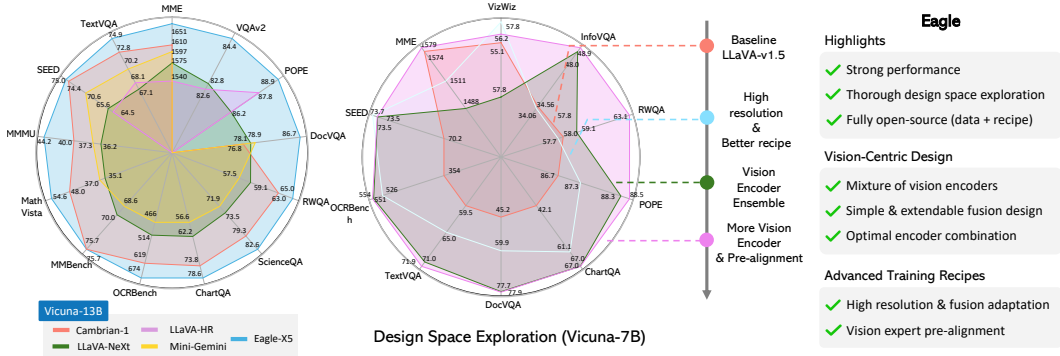


Figure 1: **Overview of *Eagle*.** *Eagle* is a family of multimodal large language models (MLLMs) with a mixture of vision encoders. Left: comparisons between *Eagle* and existing competitive MLLMs with *Vicuna-13B* (Chiang et al., 2023), with *Eagle* achieving favorable results on all 13 benchmarks. Middle: an evolutionary road map of the design space and advanced training recipes leading to consistent and significant improvements. Right: highlights and core features of *Eagle*.

ABSTRACT

The ability to accurately interpret complex visual information is a crucial topic of multimodal large language models (MLLMs). Recent work indicates that enhanced visual perception significantly reduces hallucinations and improves performance on resolution-sensitive tasks, such as optical character recognition and document analysis. A number of recent MLLMs achieve this goal using a mixture of vision encoders. Despite their success, there is a lack of systematic comparisons and detailed ablation studies addressing critical aspects, such as expert selection and the integration of multiple vision experts. This study provides an extensive exploration of the design space for MLLMs using a mixture of vision encoders and resolutions. Our findings reveal several underlying principles common to various existing strategies, leading to a streamlined yet effective design approach. We discover that simply concatenating visual tokens from a set of complementary vision encoders is as effective as more complex mixing architectures or strategies. We additionally introduce *Pre-Alignment* to bridge the gap between vision-focused encoders and language tokens, enhancing model coherence. The resulting family of MLLMs, *Eagle*, surpasses other leading open-source models on major MLLM benchmarks.

1 INTRODUCTION

The success of large language models (LLMs) has triggered significant interest in enabling their visual perception capability, such that they could see, understand, and reason in the real world. At the center of these multimodal large language models (MLLMs) (Fei et al., 2024) is a typical design

*Equal contribution. Work done during an internship at NVIDIA.

†Equal advising. Corresponding authors: {guilinl, zhidingy}@nvidia.com.

where images are converted into a series of visual tokens by the vision encoders and appended with the text embeddings. *CLIP* (Radford et al., 2021) is often chosen as the vision encoder since its visual representation is aligned with the text space by pre-training on image-text pairs. Depending on the architectures, training recipes, and the way how vision tokens are injected into the language model, there exist various notable families of MLLMs such as *Flamingo* (Alayrac et al., 2022), *BLIP* (Li et al., 2022; 2023d; Dai et al., 2024), *PaLI* (Chen et al., 2023e), *PaLM-E* (Driess et al., 2023) and *LLaVA* (Liu et al., 2023d;c). Most of these works keep relatively low input resolutions due to the limits on pre-trained vision encoders and LLM sequence length.

Recent studies (Li et al., 2024c; Liu et al., 2024a) show that stronger vision encoder design is important for mitigating MLLM hallucinations (Liu et al., 2023a; Wu et al., 2024) and improving resolution-sensitive tasks like optical character recognition (OCR). A constellation of works thus focuses on enhancing the capability of the vision encoder. For example, scaling up the pre-training data and parameters of vision encoder (Chen et al., 2023f) or dividing images into low-resolution patches (Liu et al., 2024a; Shi et al., 2024). However, these approaches usually introduce large training resources. An efficient yet powerful strategy is to mix visual encoders pre-trained with different tasks and input resolutions, either fusing higher resolution encoders with the *CLIP* encoder (Luo et al., 2024; Li et al., 2024b), sequentially appending features from different encoders (Fan et al., 2024; Lin et al., 2023b; Karamcheti et al., 2024; Tong et al., 2024), or adopting more complex fusion and routing strategies to make the best of different encoders (Lee et al., 2024; Zong et al., 2024). In addition, Prismatic VLM (Liu et al., 2024b) incorporates multiple vision encoders with channel concatenation as part of their design space exploration. These “mixture-of-vision-experts” strategies are shown to be effective. However, a detailed study focusing on their designs is still lacking.

To address the above questions, our work systematically investigates the mixture-of-vision-encoders design space for improved MLLM perception. As shown in Fig. 1, our exploration of the design space consists of the following steps: 1) Benchmarking various vision encoders and searching recipes for higher resolution adaptation; 2) “Apples to apples” comparison between vision encoder fusion strategies; 3) Progressive identification of the optimal combination of multiple vision encoders; 4) Improved vision expert pre-alignment and data mixture. Our study covers the performance of vision encoders pre-trained on different tasks and resolutions (e.g., vision-language alignment (Ilharco et al., 2021; Cherti et al., 2023; Radford et al., 2021; Schuhmann et al., 2022), self-supervised learning (Oquab et al., 2023), detection (Fang et al., 2023b;a), segmentation (Kirillov et al., 2023), and OCR (Lee et al., 2023)). We use a round-robin approach to incorporate additional vision experts. Starting with the basic *CLIP* (Radford et al., 2021) encoder, we add one additional expert each time with the best improvement in each round.

Our work is not the first one to leverage multiple vision encoders in MLLM. However, the systematic study leads to several interesting new findings under this setting:

- Unlocking the vision encoders during MLLM training matters. This is in sharp contrast to the LLaVA (Liu et al., 2023d;c) family and many works that consider multiple vision encoders or teachers (Lin et al., 2023b; Liu et al., 2024b; Fan et al., 2024; Kar et al., 2024; Ranzinger et al., 2024; Lee et al., 2024), where freezing the vision encoders has been a common choice.
- Some recently proposed fusion strategies (Luo et al., 2024; Li et al., 2024b) do not show significant advantages despite their advanced designs. Instead, we find that straightforward channel concatenation stands out as a simple yet competitive fusion strategy, offering the best efficiency and performance.
- Incorporating additional vision experts leads to consistent gain, making it a promising path to systematically enhance MLLM perception besides scaling up vision encoders. The improvement is particularly pronounced when vision encoders are unlocked.
- We propose a pre-alignment stage where non-text-aligned vision experts are individually fine-tuned with a frozen LLM before being trained together. This stage is found to enhance the MLLM performance significantly under the mixture-of-vision-encoder design.

We finally conclude our findings into a family of MLLMs termed *Eagle*. *Eagle* is evaluated on a series of benchmarks, including visual question answering, OCR/document-related tasks, and benchmarks tailored for MLLMs. Our model attains state-of-the-art performance across different benchmarks and demonstrates obvious advantages on OCR and document understanding tasks. Using

the same pre-train and supervised fine-tuning data from *Cambrian-1* (Tong et al., 2024) - a concurrent family of vision-centric MLLMs sharing similar design spirits, *Eagle* models overall achieve better performance. We hope that the *Eagle* can provide a highly performant and easy-to-reproduce MLLM solution to the community.

2 DESIGN SPACE EXPLORATION

In this section, we show how to utilize the advantages of different vision encoders via step-by-step investigations, yielding the *Eagle* model family. Unlike previous methods focusing on new fusion strategies or architectures among vision encodes, our goal is to identify a set of minimalistic design to fuse different vision encoders supported with detailed ablations, removing any unnecessary parts. As shown in Fig. 2, we start by extending the basic *CLIP* encoder (Radford et al., 2021) to a set of vision experts with different architectures, pre-training tasks, and resolutions. With these experts, we then compare different fusion architectures and methods and study how to optimize the pre-training strategies given more encoders. We also give a detailed analysis of how to select the vision encoders to be integrated. Finally, we put all the findings together and further extend to multiple expert vision encoders with different resolutions and domain knowledge.

2.1 BASE SETUP

We adopt *LLaVA-1.5*'s (Liu et al., 2023c) model architecture as the basis, which consists of a large language model (Vicuna-v1.5 7B (Chiang et al., 2023)), a vision encoder, and a projection layer. The projection layer projects the visual embedding from the vision encoder into the text embedding space.

Base training data. We adopt the same pre-training data (**LLaVA-595k**) as *LLaVA-1.5* (Liu et al., 2023c) for the first pre-training stage, which consists of 595k image text pairs. To fully examine the potential of different vision experts and fusion methods, instead of using the SFT data from *LLaVA-1.5* (Liu et al., 2023c), we collect data from a series of tasks and convert them into multimodal conversations for the supervised fine-tuning (SFT) stage, denoted as **Eagle1.8M** in Table 1.

Table 1: Composition of the base supervised fine-tuning data (Eagle1.8M).

| Total Data Size | Data Source |
|-----------------|--|
| 1,809k | <i>LLaVA-1.5</i> (665k) (Liu et al., 2023c), DocVQA (39k) (Mathew et al., 2021), synDog-EN (50k) (Kim et al., 2022), ChartQA (28k) (Masry et al., 2022), DVQA (25k) (Kafle et al., 2018), AI2D (15k) (Kembhavi et al., 2016a), ShareGPT-4V (100k) (Chen et al., 2023b), laion-GPT4V (11k) (lai, 2023), LVIS-Instruct4V (220k) (Wang et al., 2023a), LRV-Instruct (150k) (Liu et al., 2023b), Geo170k (120k) (Gao et al., 2023), LLaVAR (20k) (Zhang et al., 2023), Visual7W (70k) (Zhu et al., 2016), Open-Hermes 2.5 (300k) (Teknium, 2023) |

Base training recipes. We start from the *LLaVA-1.5* (Liu et al., 2023c) recipe where the model is first pre-trained with image-text pairs for one epoch with a batch size of 256. The whole model is frozen and only the projector layer is updated in this pre-training stage. In the second stage, we further fine-tune the model on the multi-modal conversation data for one epoch with a batch size of 128. The learning rates are set to be $1e-3$ for the first stage and $2e-5$ for the second stage, respectively.

Base evaluation. To conduct a comprehensive comparison of various methods, we adopt 11 distinct benchmarks that span multiple tasks. These benchmarks include 1) **General VQA tasks**: GQA (Hudson & Manning, 2019), VizWiz (Gurari et al., 2018), MME (Fu et al., 2023), SEED (Li et al., 2023c); 2) **OCR/document/chart understanding**: OCRBench (Liu et al., 2023f), DocVQA (Mathew et al., 2021), ChartQA (Masry et al., 2022); 3) **vision-centric tasks**: POPE (Li et al., 2023e), Real-WorldQA (xAI, 2024); 4) **knowledge-based tasks**: ScienceQA (Saikh et al., 2022), AI2D (Kembhavi et al., 2016b). To obtain an average score, we normalize each benchmark to a total score of 1,000 and then calculate the average score across all benchmarks.

2.2 STRONGER *CLIP* ENCODER

We start our exploration by upgrading the vanilla *CLIP* Radford et al. (2021) model since it has become a standard choice for most of the MLLMs Liu et al. (2023d;c). While *CLIP* models are known to benefit multimodal tasks via the text-image alignment, they also have inherent drawbacks. For instance, many existing MLLMs (Liu et al., 2023c) tend to use the pre-trained *CLIP* resolutions (such as 224×224 or 336×336) as their input resolutions. In these cases, the encoders often fail to capture fine-grained details that are important for resolution-sensitive tasks like OCR and document understanding (Li et al., 2024c).

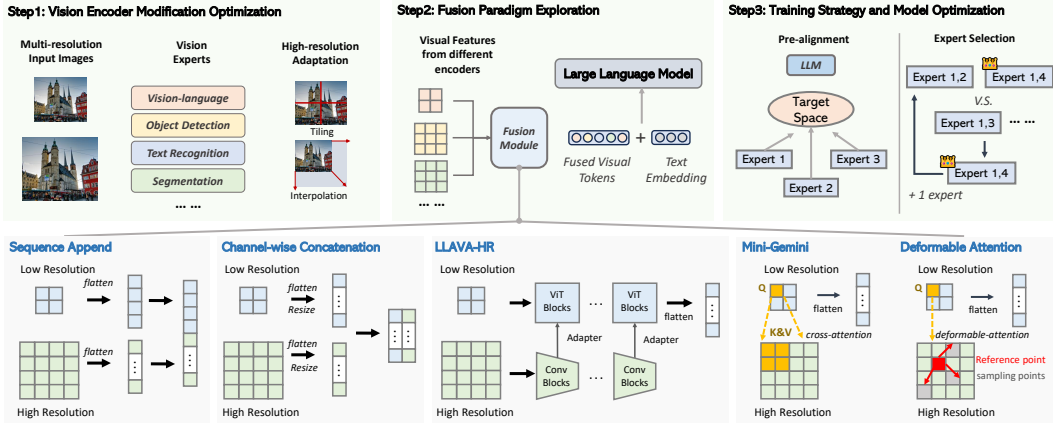


Figure 2: **Overview of the *Eagle* exploration.** In this work, we explore the design space of Multi-Modal Large Language Models (MLLMs) with multiple vision encoders, aiming to identify optimized design choices and enhance MLLM perception. We collect a range of vision experts and adapt them for integration into MLLMs. A systematic comparison of popular fusion paradigms is then conducted under controlled settings. After identifying discrepancies between vision experts pre-trained on different tasks, we optimize the pre-training strategy through a pre-alignment stage and use round-robin searching to determine the optimal combination of vision encoders.

To handle increased input resolution, a common practice is to use tiling where input images are divided into tiles and encoded separately (Liu et al., 2024a; Li et al., 2024c), or just interpolate the position embedding of the vision transformer model to fit high-resolution inputs (Chen et al., 2023c;d; Beyer et al., 2024). We compare these two approaches with frozen/unfrozen vision encoders under different resolutions, with the results shown in Table 2. Our findings can be summarized as follows:

- Updating the *CLIP* encoder during SFT significantly improves performance at higher resolutions but slightly reduces it when using the pre-training resolution.
- Interpolating *CLIP* encoder to fit the input size of 448×448 offers a strong balance between efficiency and performance, trailing the 672×672 version with less than half the tokens.
- Despite its smaller size (0.3B vs. 5.9B) and less pre-training data, the *CLIP* encoder gets close with interpolation approaches *InternVL*’s (Chen et al., 2023f) performance under the same setting.

Based on the results, we can see that *Direct interpolation* to 448×448 can achieve competitive performance while being more efficient. We thus use the *CLIP* encoder with a 448×448 input resolution while unlocking the encoder during the SFT stage.

2.3 VISION EXPERTS

To better establish the foundation for multi-vision expert fusion, we extend the toolbox with vision experts pre-trained on different tasks and resolutions, and verify our findings on high-resolution adaptation with these experts. This also helps us identify the distinct advantages of different experts. We collect a set of vision experts, including: (1) *Vision-Language Alignment*: *CLIP* (Radford et al., 2021) and *ConvNeXt* (Liu et al., 2022) from *OpenCLIP* (Ilharco et al., 2021; Schuhmann et al., 2022). (2) *Object-Centric*: *EVA-02* (Fang et al., 2023b;a) pre-trained on detection datasets. (3) *OCR*: *Pix2Struct* (Lee et al., 2023). (4) *Segmentation*: *SAM* (Kirillov et al., 2023). (5) *Self-supervised*: *DINOv2* (Oquab et al., 2023). We resize the output 2D feature maps of each vision encoder using bilinear interpolation or pixel shuffle (Shi et al., 2016) to ensure that the visual token number equals 1024.

Table 2: **Comparing different high-resolution adaption methods.** “#Tok(V)” denotes the number of visual tokens. “#Params”, “FLOPs” and “Img/Sec” denote the model size, complexity and throughput (bs=4) of the vision encoder.

| Method | Unfreeze | Res. | #Tok(V) | #Params | FLOPs | Img/Sec | Avg. |
|--------------------|----------|------|---------|---------|-------|---------|-------|
| <i>Original</i> | ✗ | | 336 | 576 | 0.3B | 119G | 197.2 |
| <i>Original</i> | ✓ | | 336 | 576 | 0.3B | 119G | 197.2 |
| <i>Interpolate</i> | ✗ | | 448 | 1024 | 0.3B | 214G | 119.5 |
| <i>Interpolate</i> | ✓ | | 448 | 1024 | 0.3B | 214G | 119.5 |
| <i>Interpolate</i> | ✓ | | 672 | 2304 | 0.3B | 480G | 56.3 |
| <i>Tiled-input</i> | ✓ | | 672 | 2304 | 0.3B | 476G | 51.6 |
| <i>InternVL</i> | ✗ | | 448 | 1024 | 5.9B | 5669G | 13.52 |
| <i>InternVL</i> | ✓ | | 448 | 1024 | 5.9B | 5669G | 13.52 |

Results in Table 3 show that unfreezing the vision experts again leads to consistent improvement, which is aligned with Sec. 2.2. In addition, results in Table 10 (see Appendix A.1) further demonstrate that *MLLMs with these task-specific vision encoders achieve optimal performance in their pre-training domains*. EVA-02 excels in the object hallucination evaluation benchmark POPE and general visual question answering benchmark GQA. CLIP and ConvNeXt perform well across all benchmarks, benefiting from their training on large-scale image-text pairs using contrastive loss. Conversely, while Pix2Struct excels in text recognition, it shows limited capability in object recognition and general VQA tasks, like POPE and GQA. DINOv2 and SAM, pre-trained with self-supervised learning and segmentation, struggle with text recognition tasks.

Table 3: Comparison between different vision experts as the MLLM encoders.

| Category | Vision Encoder | Res. | Post-process | Unfreeze | Avg. | Model Link |
|------------------|----------------|------|-----------------|----------|--------------|---------------------|
| VL Alignment | ConvNeXt | 1024 | None | ✗ | 654.6 | ConvNeXt-XXL |
| | | | | ✓ | 682.1 | |
| Segmentation | SAM | 1024 | Pixel Unshuffle | ✗ | 486.2 | SAM-ViT-Large |
| | | | | ✓ | 510.5 | |
| Object Detection | EVA-02 | 1024 | Resize | ✗ | 543.7 | EVA-02-L-Det |
| | | | | ✓ | 639.1 | |
| Text Recognition | Pix2Struct | 1024 | Resize | ✗ | 598.6 | Pix2Struct-02-Large |
| | | | | ✓ | 606.2 | |
| Self-Supervised | DINOv2 | 448 | None | ✗ | 520.7 | ViT-L/14-Reg |
| | | | | ✓ | 537.3 | |

2.4 FUSION STRATEGY

Existing MLLM frameworks have proposed various mixture-of-vision-encoder strategies, with the hope that their domain-specific strengths can be leveraged. In all cases, improvements in MLLM performance have been reported with the fusion of vision encoders. However, the roles of the fusion strategies as part of their MLLM architecture innovations, have not been decoupled and clearly studied under an “apples to apples” comparison. It is thus not entirely clear how much improvement is from the fusion strategies themselves versus the improved representations from various encoders.

We notice that existing popular fusion strategies, despite their variations in designs, can be broadly represented by the following several categories: (1) *Sequence Append*: directly appending the visual tokens from different backbones as a longer sequence (Fan et al., 2024; Kar et al., 2024); (2) *Channel Concatenation*: concatenating the visual tokens along the channel dimension without increasing the sequence length (Lin et al., 2023b; Karamcheti et al., 2024); (3) *LLaVA-HR*: injecting high-resolution features into low-resolution vision encoders using mixture-of-resolution adapter (Luo et al., 2024); (4) *Mini-Gemini*: using the CLIP tokens as the low-resolution queries to cross-attend another high-resolution vision encoder in the co-located local windows (Li et al., 2024b). (5) *Deformable Attention*: a new baseline we introduce on top of *Mini-Gemini*, where the vanilla window attention is replaced with deformable attention (Zhu et al., 2021). Fig. 2 gives a detailed illustration of these fusion strategies. To better study them, we choose “CLIP+ConvNeXt” and “CLIP+ConvNeXt+SAM” as the base multi-encoder combinations to perform comparisons.

Our study in Table 4 shows that *Channel Concatenation* stands out with the best performance, expandability, and efficiency. The “injection-based” methods, such as *LLaVA-HR*, *Mini-Gemini* and *Deformable Attention*, are in general less competitive on TextVQA (Singh et al., 2019) and OCR-Bench (Liu et al., 2023f), performing worse than using ConvNeXt alone as the vision encoder. Although sequence append shows comparable performance to channel concatenation, it faces the challenge of handling significantly increased sequence lengths with additional vision encoders.

Table 4: Comparison of different fusion methods for different vision experts. “#Token(V)” denotes the number of visual tokens. “#Tokens/s” denotes the inference throughput of the whole pipeline.

| Vision Encoders | Fusion | #Token(V) | #Tokens/s | #Params | Avg. |
|-----------------------|------------------|-----------|-------------|--------------|--------------|
| CLIP + ConvNeXt | Seq. Append | 2048 | 46.1 | 1200M | 690.5 |
| | Channel Concat. | 1024 | 47.3 | 1184M | 681.5 |
| | LLaVA-HR | 1024 | 47.0 | 1219M | 678.7 |
| | Mini-Gemini | 1024 | 45.3 | 1201M | 672.5 |
| | Deformable Attn. | 1024 | 47.3 | 1201M | 674.3 |
| CLIP + ConvNeXt + SAM | Seq. Append | 3072 | 40.3 | 1529M | 686.2 |
| | Channel Concat. | 1024 | 46.3 | 1495M | 690.4 |

2.5 VISON-LANGUAGE PRE-ALIGNMENT

As shown in Table 3, encoders pre-trained exclusively on vision tasks (e.g., detection, OCR, and segmentation) are less competitive compared to those pre-trained on vision language alignment. This is possibly due to representational inconsistencies when integrated with large language models.

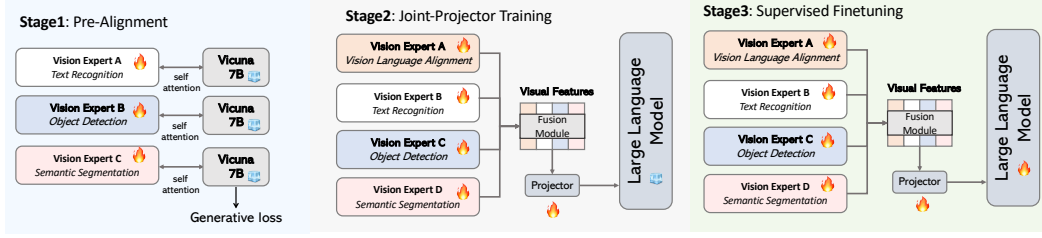


Figure 3: **The proposed training strategy of Eagle.** It consists of three progressive stages, including *vision-language pre-alignment training*, *joint-project training* and *supervised fine-tuning*. These stages effectively leverage public data from diverse sources, ranging from noisy image-text pairs on the web to high-quality caption, VQA, and multimodal dialogue datasets.

Additionally, when combining different encoders, there is a gap between these encoders, creating difficulties in the training process. To address this feature inconsistency, we propose a *Pre-Alignment* training stage that first aligns each individual vision encoder with the same large language model, fostering better synergy between visual and linguistic capabilities.

Fig. 3 depicts our pre-alignment strategy. Instead of training a projector to simultaneously align multiple vision experts as in LLaVA’s (Liu et al., 2023c) original pre-training strategy, we first align the representation of each individual expert with a smaller language model (Vicuna-7B in practice) using next-token-prediction supervision. As shown in Fig. 3, with pre-alignment, the whole training process consists of three steps: 1) *training each pre-trained vision expert with their own projector, while keeping the language model frozen*; 2) *combining all vision experts from the first step and training both the projector and vision experts*; 3) *training the whole model on SFT data*.

To verify the proposed method, we compare the pre-alignment strategy with the normal two-stage training strategy in Table 5, considering both freezing and unfreezing vision experts for comparison. As shown in Table 5, although unfreezing the vision experts during SFT helps improve performance by updating the vision experts to fit the language model, the *Pre-Align* strategy more effectively mitigates the inherent biases of each vision expert and stabilizes the training process, subsequently improving overall performance.

2.6 EXTENSION TO MULTI-EXPERTS

With the optimized strategies and training recipes of incorporating individual vision experts, we consider the incorporation of even more vision experts to push the limit. To conduct the search in a systematic manner, we adopt a step-by-step greedy strategy to incorporate additional vision experts.

We consider the vision experts discussed in Section 2.3 for experiments. We mark *CLIP*, *ConvNeXt*, *SAM*, *DINOv2*, *Pix2Struct*, and *EVA-02-L* as *CL*, *CN*, *SA*, *DI*, *PS*, and *EV*, respectively. A round-robin scheme, as shown in Fig. 4, is adopted. We first use the two top-performing vision encoders, *CLIP* and *ConvNeXt*, as the basis and gradually add one more vision encoder each time. In each round, the best-performing vision encoder combination is retained for the next round.

Fig. 4 reveals several insights. Generally, **introducing additional vision encoders enhances the performance**. This indicates that the distinct advantages of different encoders can be preserved and utilized; for example, integrating the *EVA-02* encoder improves metrics on the POPE benchmark. Although individual metrics may vary, the aggregated performance shows an upward trend, as evidenced by normalized average metrics, suggesting that the overall efficacy of the system is enhanced with more encoders. Also, Fig. 4 shows that the best combination of vision experts are *CLIP*, *ConvNeXt*, *SAM*, *Pix2Struct*, and *EVA-02*. We will use this recipe in the final model.

Table 5: **The effectiveness of Pre-alignment.**

| | CLIP | Vision Expert (X) | Unfreeze | Pre-align | Avg. |
|----------|-----------------|-------------------|----------|-----------|--------------|
| CLIP-448 | SAM-1024 | | ✗ | ✗ | 630.6 |
| | | | ✗ | ✓ | 648.5 |
| | | | ✓ | ✗ | 662.5 |
| | | | ✓ | ✓ | 672.3 |
| CLIP-448 | ConvNext-1024 | | ✗ | ✗ | 652.0 |
| | | | ✗ | ✓ | 670.1 |
| | | | ✓ | ✗ | 681.5 |
| | | | ✓ | ✓ | 686.2 |
| CLIP-448 | Pix2Struct-1024 | | ✗ | ✗ | 653.5 |
| | | | ✗ | ✓ | 665.7 |
| | | | ✓ | ✗ | 673.7 |
| | | | ✓ | ✓ | 680.4 |
| CLIP-448 | EVA-02-L-1024 | | ✗ | ✗ | 630.2 |
| | | | ✗ | ✓ | 645.2 |
| | | | ✓ | ✗ | 659.2 |
| | | | ✓ | ✓ | 668.2 |

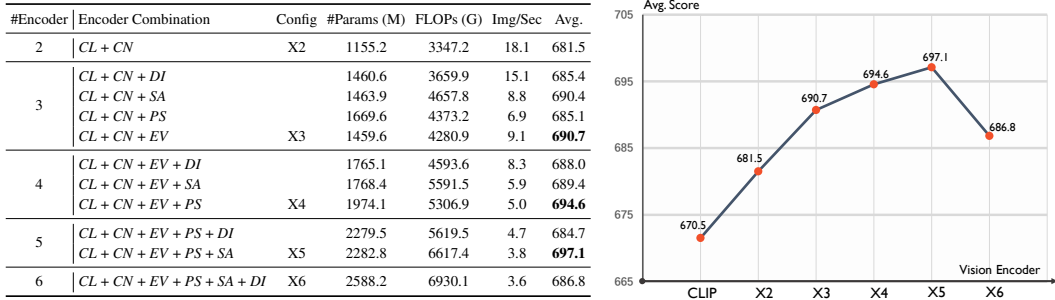


Figure 4: **Results of vision expert selection process.** CL, CN, EV, PS, SA and DI denote CLIP, ConvNeXt, EVA-02, Pix2Struct, SAM and DINOv2, respectively. (Left) The performance of various vision encoder combinations is presented, highlighting how different pairings influence overall effectiveness. “#Params”, “FLOPs” and “Img/Sec” denote the model size, complexity and throughput (bs=4) of the vision encoder. (Right) The curve illustrates the average score as the number of vision encoders increases. Each point on the curve represents the best-performing combination for the corresponding number of vision encoders. No *Pre-Alignment* is used in this comparison.

3 EXPERIMENTS

In this section, we take the findings and the best-explored design from Section 2 and compare them against the current state-of-the-art MLLMs on different tasks.

3.1 IMPLEMENTATION DETAILS

Language models. We use Vicuna-v1.5-7B (Chiang et al., 2023), Llama3-8B (AI@Meta, 2024) and Vicuna-v1.5-13B (Chiang et al., 2023) as the language models.

Vision encoders. We follow the best X4 and X5 configurations, where the interpolated CLIP-448 and pre-aligned vision experts are channel-concatenated, and trained following the exact best training recipes in Figure 3 and Table 5.

Training recipe. On Eagle1.8M, we follow the base recipe in Section 2.1 with encoder learning rate the same as SFT (2e-5). On Cambrian data, we follow Tong et al. (2024) with PT/SFT bs=1024.

3.2 MAIN RESULTS

Evaluation on visual question answering tasks. We compare Eagle model series across three Visual Question Answering (VQA) benchmarks, including GQA (Hudson & Manning, 2019), VQAv2 (Goyal et al., 2017) and VizWiz (Gurari et al., 2018). As shown in Table 6, Eagle-X5 achieves state-of-the-art performance on GQA and VQAv2, underscoring the advantages with additional vision experts.

Evaluation on OCR and chart understanding tasks. To evaluate the OCR, document, and chart understanding capabilities of Eagle, we benchmark our model on OCRBench (Liu et al., 2023f), TextVQA (Singh et al., 2019), and ChartQA (Masry et al., 2022). As illustrated in Table 6, our model significantly surpasses competitors on TextVQA, benefiting from its high-resolution architecture and integration of different vision encoders. Notably, Eagle maintains a straightforward design, supporting up to 1024x1024 resolution without requiring complex tile decomposition of images.

Fig. 5 shows some examples of OCR and document understanding cases. With high-resolution adaptation and more vision experts, our model can identify small text within images and accurately extract information according to the users’ instructions. To better understand the benefits of introducing experts pre-trained on other vision tasks, we visualize the results of a model with only the ConvNeXt and CLIP vision encoders, compared to the results of Eagle-X5 in Fig. 5. With the full set of vision encoders, the model can successfully correct mistakes, showing that even when equipped with high-resolution vision encoders pre-trained on vision-language alignment, the model’s abilities can still be enhanced by integrating additional vision experts pre-trained on diverse vision tasks.

Table 6: Main results with base training data. SQA^I denotes image split of ScienceQA.

| | Model | MME | MMB | SEED | MathVista | MMMU | POPE | SQA ^I | GQA | VizWiz | VQA2 | OCR | TextVQA | ChartQA |
|---------------------|--------------------------------|-------------|-------------|-------------|-------------|-------------|-------------|------------------|--------------|--------------|--------------|------------|-------------|-------------|
| Vicuna-7B & Qwen-7B | LLaVA-1.5 (Liu et al., 2023c) | 1510 | 64.3 | 58.6 | - | - | 85.9 | 66.8 | 62.0* | 50.0 | 78.5* | 297 | 58.2 | - |
| | LLaVA-NeXt (Liu et al., 2024a) | 1519 | 67.4 | 70.2 | 34.6 | 35.8 | 86.5 | 70.1 | 64.2* | 57.6 | 80.0* | 490 | 64.9 | - |
| | InternVL (Chen et al., 2023f) | 1525 | - | 65.4 | - | - | 86.4 | - | 62.9* | 52.5 | 79.3* | - | 57.0 | - |
| | LLaVA-HR (Luo et al., 2024) | 1554 | - | 64.2 | - | - | 87.6 | 65.1 | 64.2* | 48.7 | 81.9* | - | 67.1 | - |
| | Monkey (Li et al., 2024c) | - | - | - | - | - | - | - | 60.7* | 61.2* | 80.3* | 514 | 67.6 | 65.1 |
| | Mini-Gemini (Li et al., 2024b) | 1523 | 65.8 | - | 32.2 | 36.8 | - | 71.1 | 64.5* | - | - | 477 | 65.2 | - |
| | Eagle-X5 | 1528 | 68.4 | 73.9 | 37.0 | 36.3 | 88.8 | 70.0 | 64.9* | 54.4 | 83.4* | 529 | 71.2 | 67.7 |
| | Eagle-X5 (+Pre-Align) | 1582 | 69.7 | 73.7 | 38.2 | 38.0 | 88.7 | 71.9 | 64.6* | 58.7 | 83.6* | 566 | 71.9 | 69.3 |
| Vicuna-13B | LLaVA-1.5 (Liu et al., 2023c) | 1531 | 67.7 | 61.6 | - | 36.4 | 85.9 | 71.6 | 63.3* | 53.6 | 80.0* | 331 | 61.3 | - |
| | LLaVA-NeXt (Liu et al., 2024a) | 1575 | 70.0 | 71.9 | 35.3 | 36.2 | 86.2 | 73.5 | 65.4* | 60.5 | 82.8* | 514 | 67.1 | 62.2 |
| | InternVL (Chen et al., 2023f) | 1546 | - | - | - | - | 87.1 | - | 63.9* | 54.6 | 80.2* | 517 | 58.7 | - |
| | LLaVA-UHD (Xu et al., 2024) | 1535 | 68.0 | - | - | - | 89.1 | 72.0 | 65.2* | 56.1 | 81.7* | - | 67.7 | - |
| | LLaVA-HR (Luo et al., 2024) | 1540 | - | 64.5 | - | - | 87.8 | 68.1 | 64.8* | 57.9 | 82.6* | - | 68.1 | - |
| | Mini-Gemini (Li et al., 2024b) | 1565 | 68.6 | 70.6 | 37.0 | 37.3 | - | 71.9 | 65.8* | - | - | 466 | 65.9 | 56.6 |
| | Eagle-X5 | 1609 | 69.2 | 74.1 | 38.8 | 36.6 | 87.8 | 72.7 | 66.2* | 59.3 | 83.8* | 574 | 74.2 | 69.9 |
| | Eagle-X5 (+Pre-Align) | 1605 | 71.6 | 74.9 | 42.7 | 38.5 | 89.2 | 75.5 | 64.6* | 60.9 | 84.5* | 598 | 73.3 | 72.1 |

Evaluation on multimodal benchmarks. We evaluate *Eagle* on seven benchmarks for MLLMs to demonstrate its capabilities from different perspectives, including MME (Fu et al., 2023), MM-Bench (Liu et al., 2023e), SEED (Li et al., 2023c), MathVista (Lu et al., 2024), MMMU (Yue et al., 2024), ScienceQA (Saikh et al., 2022), and POPE (Li et al., 2023e). Specifically, MME, MMBench, and SEED assess the overall performance on various real-world tasks based on reasoning, recognition, knowledge, and OCR. MMMU focuses on challenging problems from diverse domains that require college-level knowledge. POPE evaluates the visual hallucinations of MLLMs. The metrics used in our paper adhere to the default settings of these benchmarks. We report the perception score for MME, the en_dev split for MMBench, the image split of SEED, the test-mini split of MathVista, the val split of MMMU, the F1-score of POPE, and the image split of SQA to align with the reported scores from other models.

From the data presented in Table 6, *Eagle* consistently surpasses existing models across various MLLMs on SEED and MME, demonstrating the comprehensive knowledge and reasoning abilities of *Eagle*. With the help of vision encoders on object-centric tasks, *Eagle* also achieves the best performance on the POPE benchmark. Additionally, the *Pre-Alignment* strategy discussed in Sec. 2.5 has been found to further enhance performance when integrating multiple task-specific vision backbones.

This approach not only mitigates the inherent biases of each vision expert and the synergy between different modalities but also establishes a robust framework for multiple-expert fusion.

Study on more advanced training recipes. Table. 7 presents our step-by-step experiments to study the training recipes. We found that the best recipe is to first pre-align each vision expert on *LLaVA-595K* + *Eagle1.8M*. In the pretraining stage, we combine all vision experts from the first step and training both the projector and vision experts on *LLaVA-595K* + *Eagle1.8M*. Finally, we train the whole model on the *Eagle1.8M*.

Comparison with *Cambrian-1*. Using the same pre-training and supervised fine-tuning datasets from *Cambrian-1* (Tong et al., 2024), *Eagle* demonstrates superior performance across all the evaluated

Table 7: Comparison between different training strategies. “1 epoch” means we train *Eagle* for 1 epoch in the supervised fine-tuning stage. ‘unlock*’ means we unlock vision encoders in the pre-training stage. More details in Table. 13.

| Config Summary | Pre-align | Pre-train | Fine-tune | Avg. |
|------------------|----------------------|----------------------|-----------|--------------|
| 1 epoch | X | LLaVA-595K | Eagle1.8M | 697.1 |
| 2 epoch | X | LLaVA-595K | Eagle1.8M | 698.3 |
| 1 epoch, unlock* | X | LLaVA-595K | Eagle1.8M | 698.0 |
| 1 epoch, unlock* | X | LLaVA-595K+Eagle1.8M | Eagle1.8M | 699.5 |
| 1 epoch | Eagle1.8M | LLaVA-595K | Eagle1.8M | 706.6 |
| 1 epoch, unlock* | Eagle1.8M | LLaVA-595K | Eagle1.8M | 707.1 |
| 1 epoch, unlock* | LLaVA-595K+Eagle1.8M | LLaVA-595K | Eagle1.8M | 707.8 |
| 1 epoch, unlock* | LLaVA-595K+Eagle1.8M | LLaVA-595K+Eagle1.8M | Eagle1.8M | 708.9 |

Table 8: **Results using the same training data as *Cambrian-1*** (Tong et al., 2024). SQA^I denotes ScienceQA-IMG (Saikh et al., 2022). RWQA denotes the RealworldQA (xAI, 2024).

| Model | Knowledge | | | | | General | | | | | OCR and Chart | | | | | Vision-Centric | | |
|-------------------|-------------|------------------|-------------|-------------|-------------|-------------|-------------|-------------|-------------|-------------|---------------|-------------|-------------|-------------|-------------|----------------|-------------|-------------|
| | Avg | SQA ^I | MMU | MathVista | AI2D | Avg | MME | MMB | SEED | GQA | Avg | ChartQA | OCR | TextVQA | DocVQA | Avg | MMVP | RWQA |
| <i>Llama3-8B</i> | | | | | | | | | | | | | | | | | | |
| <i>MGM-HD</i> | 55.7 | 75.1 | 37.3 | 37.0 | 73.5 | 72.7 | 1606 | 72.7 | 73.2 | 64.5 | 62.9 | 59.1 | 47.7 | 70.2 | 74.6 | 40.4 | 18.7 | 62.1 |
| <i>Cambrian-1</i> | 61.3 | 80.4 | 42.7 | 49.0 | 73.0 | 73.1 | 1547 | 75.9 | 74.7 | 64.6 | 71.3 | 73.3 | 62.4 | 71.7 | 77.8 | 57.6 | 51.3 | 64.2 |
| <i>Eagle-X5</i> | 65.2 | 84.1 | 43.5 | 56.9 | 76.2 | 74.0 | 1587 | 75.5 | 76.5 | 64.9 | 77.0 | 80.7 | 62.6 | 76.7 | 87.1 | 59.6 | 52.0 | 67.2 |
| <i>Vicuna-13B</i> | | | | | | | | | | | | | | | | | | |
| <i>MGM-HD</i> | 54.1 | 71.9 | 37.3 | 37.0 | 70.1 | 70.7 | 1597 | 68.6 | 70.6 | 63.7 | 60.8 | 56.6 | 46.6 | 70.2 | 69.8 | 38.4 | 19.3 | 57.5 |
| <i>Cambrian-1</i> | 60.2 | 79.3 | 40.0 | 48.0 | 73.6 | 73.7 | 1610 | 75.7 | 74.4 | 64.3 | 71.3 | 73.8 | 61.9 | 72.8 | 76.8 | 52.2 | 41.3 | 63.0 |
| <i>Eagle-X5</i> | 63.8 | 82.6 | 42.2 | 54.6 | 73.8 | 74.6 | 1651 | 75.7 | 75.0 | 65.0 | 75.7 | 78.6 | 62.4 | 74.9 | 86.7 | 54.8 | 44.6 | 65.0 |
| <i>Yi-34B</i> | | | | | | | | | | | | | | | | | | |
| <i>MGM-HD</i> | 62.4 | 77.7 | 48.0 | 43.4 | 80.5 | 76.2 | 1659 | 80.6 | 75.3 | 65.8 | 68.1 | 67.6 | 51.8 | 74.1 | 78.9 | 52.3 | 37.3 | 67.2 |
| <i>Cambrian-1</i> | 67.0 | 85.6 | 49.7 | 53.2 | 79.7 | 76.8 | 1689 | 81.4 | 75.3 | 65.8 | 71.9 | 75.6 | 60.0 | 76.7 | 75.5 | 60.3 | 52.7 | 67.8 |
| <i>Eagle-X5</i> | 68.6 | 85.5 | 53.2 | 57.9 | 79.1 | 76.3 | 1677 | 81.0 | 75.6 | 64.9 | 75.4 | 77.2 | 62.4 | 78.8 | 83.0 | 59.8 | 50.0 | 69.5 |

benchmarks without bells and whistles. As shown in Table 8, *Eagle* outperforms the *Cambrian-1* counterparts considerably for the *OCR and Chart* category. Consistent improvements are also observed for the *General*, *Knowledge*, and *Vision-Centric* categories, showing the robustness and generalization ability of the improved perception design in *Eagle*.


4 RELATED WORK

Multimodal large language models. Our work is related to the general architecture design of multimodal large language models. Besides the line of representative open-source research mentioned in the introduction section, other notable families of MLLMs include, but are not limited to *MiniGPT-4* (Zhu et al., 2023; Chen et al., 2023a), *Lynx* (Zeng et al., 2023), *Otter* (Li et al., 2023b;a), *Qwen-VL* (Bai et al., 2023), *CogVLM* (Wang et al., 2023b; Hong et al., 2024), *VILA* (Lin et al., 2023a), *GPT-4V* (Achiam et al., 2023), *Gemini* (Team et al., 2023), and *Llama 3.1* (Dubey et al., 2024). Depending on how vision signals are integrated into the language model, MLLMs can be broadly categorized into “cross-modal attention” ones and “prefix-tuning” ones (Yin et al., 2024). The former injects visual information into different layers of LLMs using cross-modal attention (Alayrac et al., 2022; Li et al., 2023b), whereas the latter views the visual tokens as part of the language token sequence and directly append them with text embeddings (Liu et al., 2023d; Li et al., 2022; 2023d). Our model belongs to the prefix-tuning family by following a *LLaVA*-styled multimodal architecture. Considering that MLLM is a fast-growing field, readers are recommended to refer to more detailed studies and surveys such as Yin et al. (2024); Li et al. (2024a); Fei et al. (2024).

Vision encoder design for MLLMs. Our work is closely related to research focusing on improved vision encoder designs for MLLM. Early works (Liu et al., 2023d; Li et al., 2022) usually adopted vision encoder pre-trained on vision-language alignment tasks such as *CLIP* (Radford et al., 2021) and *EVA-CLIP* (Sun et al., 2023). Stronger vision encoders such as *SigLIP* (Zhai et al., 2023) and *InternVL* (Chen et al., 2023f) have been proposed to improve vision-language tasks with improved designs, larger model sizes, and better training recipes. Considering that the models are often pre-trained on low-resolution images and lack the ability to encode fine-grained details, higher resolution adaptation is often performed to increase the MLLM input resolution (Chen et al., 2023c;d; Beyer et al., 2024; Chen et al., 2024).

Besides higher resolution adaptation, models such as *LLaVA-NeXT* (Liu et al., 2024a), *LLaVA-UHD* (Xu et al., 2024), *Monkey* (Li et al., 2024c), *InternLM-XComposer* (Dong et al., 2024), and *InternVL* (Chen et al., 2024) use adaptive tiling to divide high-resolution input into lower resolution patches that are processed separately. Although the ability to handle higher resolution is similarly made possible with the introduction of additional vision experts, its spirit is slightly orthogonal to the tiling techniques in terms of diversifying the visual representations. Both techniques are compatible and can be combined together.


Effectiveness of more vision experts



User: Tell me the locations of all the number 10 jerseys in the picture. Answer the questions in details with a few sentences

CLIP + ConvNeXt baseline: There are two number 10 jerseys in the picture. One is on the left side of the group, and the other is on the right side

Eagle-X5: In the image, there are two players wearing jerseys with the number 10. One of them is standing in the center of the group, while the other is positioned towards the right side of the group. Both players are part of the basketball team, as indicated by their uniforms and the context of the image.



User: What's the opening time of the restaurant on Sunday?

CLIP + ConvNeXt baseline: 11:30-2:00

Eagle (more vision experts): closed

User: What's the value of the row "low" and column "referents"?

CLIP + ConvNeXt baseline: 2012-13

Eagle-X5: 10,970 (60%)

Qualitative Examples

| Electrode reaction | Standard electrode potential (V) |
|--|----------------------------------|
| $\text{Au}^{3+} + 3\text{e}^- \rightarrow \text{Au}$ | +1.420 |
| $\text{Cu}^{2+} + 2\text{e}^- \rightarrow \text{Cu}$ | +0.340 |
| $\text{Ni}^{2+} + 2\text{e}^- \rightarrow \text{Ni}$ | -0.250 |
| $\text{Fe}^{2+} + 2\text{e}^- \rightarrow \text{Fe}$ | -0.440 |
| $\text{Na}^+ + \text{e}^- \rightarrow \text{Na}$ | -2.924 |

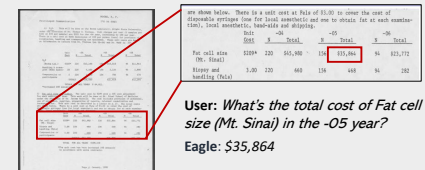
User: Below are shown, for five metals, reduction reactions and standard electrode potential values. Which of these metals is the least reactive? explain your answers in detail.

Option: (A)Au (B) Cu (C) Ni(D) Fe (E) Na

Eagle: The least reactive metal among the given options is (A) Au.

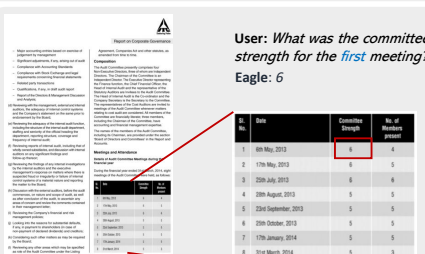
Explanation: The standard electrode potential (E°) is a measure of the tendency of a metal to lose electrons and undergo a reduction reaction. The higher the E° value, the more reactive the metal is.

In the given table, the standard electrode potential values are as follows.
(A)Au: +1.420 V (B) Cu: +0.340 V (C) Ni: -0.250V (D) Fe: -0.440V (E) Na: -2.924V
 Comparing these values, we can see that the metal with the highest E° value (+1.420 V) is Au, which indicates that it is the least reactive among the given options. The other metals have lower E° values, making them more reactive than Au.



User: What's the total cost of Fat cell size (Mt. Sinai) in the -05 year?

Eagle: \$35,864



User: What was the committee strength for the first meeting?

Eagle: 6

Figure 5: **Qualitative comparison of different numbers of vision experts.** *Baseline* means *Eagle* with only *CLIP+ConvNext*. *More Vision Experts* denotes the *Eagle-X5* model. We highlight a failure case in RED. BLUE indicates the correct answers. With more vision experts, *Eagle* can more precisely capture the information in the image and provide the correct answer.

Our work is most related to existing models using multiple vision encoders for improved perception. *Mini-Gemini* (Li et al., 2024b) and *LLaVA-HR* (Luo et al., 2024) propose to fuse high-resolution visual features into the low-resolution visual tokens. Apart from the resolution issue, these pre-trained vision encoders may lack specific abilities such as reading text and localizing objects. Hence, a series of works have integrated vision models pre-trained on different tasks for more comprehensive capabilities. For example, *Mousi* (Fan et al., 2024), *Prismatic VLM* (Karamcheti et al., 2024) and *Brave* (Kar et al., 2024) fuse visual tokens from different vision encoders by concatenating along the channel or token direction. There are also more complex approaches, including knowledge distillation Ranzinger et al. (2024), augmenting the input prompt with the information output by the vision experts (Lee et al., 2024; He et al., 2024; Liu et al., 2024b), or using a routing network to assign input to proper vision experts (Zong et al., 2024). In particular, *Prismatic VLM* (Karamcheti et al., 2024) systematically explores the design space of MLLMs across various dimensions, including data, training recipes, and notably. It also includes the vision encoder ensemble as part of its enhancement strategies. However, it lacks a comprehensive ablation study and discussion addressing the challenges associated with combining multiple vision encoders.

5 CONCLUSION

We conduct an in-depth analysis study on the design space for integrating vision encoders for multimodal large language models. Unlike previous works that focus on designing novel fusion paradigms, we find systematic design choice matters and discover a series of useful techniques. Step by step, we optimize the training recipes of individual vision encoders, identify an extendable and efficient fusion method, and gradually combine vision encoders with different domain knowledge. The results show the importance of basic design space. We hope our work can serve as a new basis and bring new inspiration for the vision encoder design for MLLM.

6 ACKNOWLEDGMENTS

The team would like to thank Yunhao Fang and Jason Lu for sharing the data and training recipes, and Yawen Luo for the assistance on figure editing. We thank Wei Ping, Zhuolin Yang, Wenliang Dai, Nayeon Lee, Boxin Wang, Ilia Karmanov, Lukas Voegtli, Philipp Fischer, Matthieu Le and Tuomas Rintamaki for their assistance on the internal codebases. We also thank the valuable discussions and input from Zhiqi Li, Guo Chen, Shilong Liu, Jihao Liu, Ming-Chang Chiu, Yunze Man, Shiyi Lan, Nadine Chang, Maying Shen, Vibashan VS, Jenny Schmalfluss, Jose Alvarez, Amala Sanjay Deshmukh, Mike Ranzinger, Greg Heinrich, Pavlo Molchanov, Vidya Murali, Parthasarathy Sriram, Mohammad Shoeybi, Song Han, Ofri Masad, Osvald Nitski, Qing Miao, Yao Xu, Jane Scowcroft, Dmitry Chichkov and Padmavathy Subramanian. Finally, the team would like to thank the Hugging Face Team that for the support of ZERO GPU demo, and the NVIDIA infrastructure team for their prompt and helpful assistance. Min Shi is partly supported by NSF Award #2427478 and #2229873.

REFERENCES

- LAION-GPT4v dataset. <https://huggingface.co/datasets/laion/gpt4v-dataset>, 2023.
- Josh Achiam, Steven Adler, Sandhini Agarwal, Lama Ahmad, Ilge Akkaya, Florencia Leoni Aleman, Diogo Almeida, Janko Altschmidt, Sam Altman, Shyamal Anadkat, et al. GPT-4 technical report. *arXiv:2303.08774*, 2023.
- AI@Meta. Llama 3 model card, 2024. URL https://github.com/meta-llama/llama3/blob/main/MODEL_CARD.md.
- Jean-Baptiste Alayrac, Jeff Donahue, Pauline Luc, Antoine Miech, Iain Barr, Yana Hasson, Karel Lenc, Arthur Mensch, Katherine Millican, Malcolm Reynolds, et al. Flamingo: a visual language model for few-shot learning. In *NeurIPS*, 2022.
- Jinze Bai, Shuai Bai, Shusheng Yang, Shijie Wang, Sinan Tan, Peng Wang, Junyang Lin, Chang Zhou, and Jingren Zhou. Qwen-VL: A frontier large vision-language model with versatile abilities. *arXiv:2308.12966*, 2023.
- Lucas Beyer, Andreas Steiner, André Susano Pinto, Alexander Kolesnikov, Xiao Wang, Daniel Salz, Maxim Neumann, Ibrahim Alabdulmohsin, Michael Tschannen, Emanuele Bugliarello, et al. Paligemma: A versatile 3b vlm for transfer. *arXiv:2407.07726*, 2024.
- Jun Chen, Deyao Zhu, Xiaoqian Shen, Xiang Li, Zechun Liu, Pengchuan Zhang, Raghuraman Krishnamoorthi, Vikas Chandra, Yunsang Xiong, and Mohamed Elhoseiny. MiniGPT-v2: Large language model as a unified interface for vision-language multi-task learning. *arXiv:2310.09478*, 2023a.
- Lin Chen, Jisong Li, Xiaoyi Dong, Pan Zhang, Conghui He, Jiaqi Wang, Feng Zhao, and Dahua Lin. ShareGPT4V: Improving large multi-modal models with better captions. *arXiv:2311.12793*, 2023b.
- Xi Chen, Josip Djolonga, Piotr Padlewski, Basil Mustafa, Soravit Changpinyo, Jialin Wu, Carlos Riquelme Ruiz, Sebastian Goodman, Xiao Wang, Yi Tay, et al. PaLI-X: On scaling up a multilingual vision and language model. *arXiv:2305.18565*, 2023c.
- Xi Chen, Xiao Wang, Lucas Beyer, Alexander Kolesnikov, Jialin Wu, Paul Voigtlaender, Basil Mustafa, Sebastian Goodman, Ibrahim Alabdulmohsin, Piotr Padlewski, et al. PaLI-3 vision language models: Smaller, faster, stronger. *arXiv:2310.09199*, 2023d.
- Xi Chen, Xiao Wang, Soravit Changpinyo, AJ Piergiovanni, Piotr Padlewski, Daniel Salz, Sebastian Goodman, Adam Grycner, Basil Mustafa, Lucas Beyer, et al. PaLI: A jointly-scaled multilingual language-image model. In *ICLR*, 2023e.
- Zhe Chen, Jiannan Wu, Wenhai Wang, Weijie Su, Guo Chen, Sen Xing, Muyan Zhong, Qinglong Zhang, Xizhou Zhu, Lewei Lu, Bin Li, Ping Luo, Tong Lu, Yu Qiao, and Jifeng Dai. InternVL: Scaling up vision foundation models and aligning for generic visual-linguistic tasks. *arXiv:2312.14238*, 2023f.

- Zhe Chen, Weiyun Wang, Hao Tian, Shenglong Ye, Zhangwei Gao, Erfei Cui, Wenwen Tong, Kongzhi Hu, Jiapeng Luo, Zheng Ma, et al. How far are we to gpt-4v? closing the gap to commercial multimodal models with open-source suites. *arXiv:2404.16821*, 2024.
- Mehdi Cherti, Romain Beaumont, Ross Wightman, Mitchell Wortsman, Gabriel Ilharco, Cade Gordon, Christoph Schuhmann, Ludwig Schmidt, and Jenia Jitsev. Reproducible scaling laws for contrastive language-image learning. In *CVPR*, 2023.
- Wei-Lin Chiang, Zhuohan Li, Zi Lin, Ying Sheng, Zhanghao Wu, Hao Zhang, Lianmin Zheng, Siyuan Zhuang, Yonghao Zhuang, Joseph E. Gonzalez, Ion Stoica, and Eric P. Xing. Vicuna: An open-source chatbot impressing gpt-4 with 90%* chatgpt quality. <https://lmsys.org/blog/2023-03-30-vicuna/>, March 2023.
- Wenliang Dai, Junnan Li, Dongxu Li, Anthony Meng Huat Tiong, Junqi Zhao, Weisheng Wang, Boyang Li, Pascale N Fung, and Steven Hoi. InstructBLIP: Towards general-purpose vision-language models with instruction tuning. In *NeurIPS*, 2024.
- Xiaoyi Dong, Pan Zhang, Yuhang Zang, Yuhang Cao, Bin Wang, Linke Ouyang, Songyang Zhang, Haodong Duan, Wenwei Zhang, Yining Li, et al. InternLM-XComposer2-4KHD: A pioneering large vision-language model handling resolutions from 336 pixels to 4k hd. *arXiv:2404.06512*, 2024.
- Danny Driess, Fei Xia, Mehdi SM Sajjadi, Corey Lynch, Aakanksha Chowdhery, Brian Ichter, Ayzaan Wahid, Jonathan Tompson, Quan Vuong, Tianhe Yu, et al. PaLM-E: An embodied multimodal language model. *arXiv:2303.03378*, 2023.
- Abhimanyu Dubey, Abhinav Jauhri, Abhinav Pandey, Abhishek Kadian, Ahmad Al-Dahle, Aiesha Letman, Akhil Mathur, Alan Schelten, Amy Yang, Angela Fan, et al. The Llama 3 herd of models. *arXiv:2407.21783*, 2024.
- Xiaoran Fan, Tao Ji, Changhao Jiang, Shuo Li, Senjie Jin, Sirui Song, Junke Wang, Boyang Hong, Lu Chen, Guodong Zheng, et al. MouSi: Poly-visual-expert vision-language models. *arXiv:2401.17221*, 2024.
- Yuxin Fang, Quan Sun, Xinggang Wang, Tiejun Huang, Xinlong Wang, and Yue Cao. EVA-02: A visual representation for neon genesis. *arXiv:2303.11331*, 2023a.
- Yuxin Fang, Wen Wang, Binhui Xie, Quan Sun, Ledell Wu, Xinggang Wang, Tiejun Huang, Xinlong Wang, and Yue Cao. EVA: Exploring the limits of masked visual representation learning at scale. In *CVPR*, 2023b.
- Hao Fei, Yuan Yao, Zhuosheng Zhang, Fuxiao Liu, Ao Zhang, and Tat-Seng Chua. From multimodal llm to human-level ai: Modality, instruction, reasoning, efficiency and beyond. In *LREC-Coling Tutorials*, 2024.
- Chaoyou Fu, Peixian Chen, Yunhang Shen, Yulei Qin, Mengdan Zhang, Xu Lin, Zhenyu Qiu, Wei Lin, Jinrui Yang, Xiawu Zheng, et al. MME: A comprehensive evaluation benchmark for multimodal large language models. *arXiv:2306.13394*, 2023.
- Jiahui Gao, Renjie Pi, Jipeng Zhang, Jiacheng Ye, Wanjuan Zhong, Yufei Wang, Lanqing Hong, Jianhua Han, Hang Xu, Zhenguang Li, and Lingpeng Kong. G-llava: Solving geometric problem with multi-modal large language model. *arXiv:2312.11370*, 2023.
- Yash Goyal, Tejas Khot, Douglas Summers-Stay, Dhruv Batra, and Devi Parikh. Making the V in VQA matter: Elevating the role of image understanding in Visual Question Answering. In *CVPR*, 2017.
- Danna Gurari, Qing Li, Abigale J. Stangl, Anhong Guo, Chi Lin, Kristen Grauman, Jiebo Luo, and Jeffrey P. Bigham. Vizwiz grand challenge: Answering visual questions from blind people. In *CVPR*, 2018.
- Xin He, Longhui Wei, Lingxi Xie, and Qi Tian. Incorporating visual experts to resolve the information loss in multimodal large language models. *arXiv:2401.03105*, 2024.

- Wenyi Hong, Weihang Wang, Qingsong Lv, Jiazheng Xu, Wenmeng Yu, Junhui Ji, Yan Wang, Zihan Wang, Yuxiao Dong, Ming Ding, et al. CogAgent: A visual language model for gui agents. In *CVPR*, 2024.
- Drew A Hudson and Christopher D Manning. GQA: A new dataset for real-world visual reasoning and compositional question answering. In *CVPR*, 2019.
- Gabriel Ilharco, Mitchell Wortsman, Ross Wightman, Cade Gordon, Nicholas Carlini, Rohan Taori, Achal Dave, Vaishaal Shankar, Hongseok Namkoong, John Miller, Hannaneh Hajishirzi, Ali Farhadi, and Ludwig Schmidt. Openclip, July 2021. URL <https://doi.org/10.5281/zenodo.5143773>. If you use this software, please cite it as below.
- Kushal Kafle, Scott Cohen, Brian Price, and Christopher Kanan. DVQA: Understanding data visualizations via question answering. In *CVPR*, 2018.
- Oğuzhan Fatih Kar, Alessio Tonioni, Petra Poklukar, Achin Kulshrestha, Amir Zamir, and Federico Tombari. BRAVE: Broadening the visual encoding of vision-language models. *arXiv:2404.07204*, 2024.
- Siddharth Karamcheti, Suraj Nair, Ashwin Balakrishna, Percy Liang, Thomas Kollar, and Dorsa Sadigh. Prismatic vlms: Investigating the design space of visually-conditioned language models. *arXiv:2402.07865*, 2024.
- Aniruddha Kembhavi, Michael Salvato, Eric Kolve, Minjoon Seo, Hannaneh Hajishirzi, and Ali Farhadi. A diagram is worth a dozen images. *arXiv:1603.07396*, 2016a.
- Aniruddha Kembhavi, Mike Salvato, Eric Kolve, Min Joon Seo, Hannaneh Hajishirzi, and Ali Farhadi. A diagram is worth a dozen images. In *Computer Vision - ECCV 2016 - 14th European Conference, Amsterdam, The Netherlands, October 11-14, 2016, Proceedings, Part IV*, volume 9908 of *Lecture Notes in Computer Science*, pp. 235–251, 2016b.
- Geewook Kim, Teakgyu Hong, Moonbin Yim, JeongYeon Nam, Jinyoung Park, Jinyeong Yim, Wonseok Hwang, Sangdoo Yun, Dongyoon Han, and Seunghyun Park. OCR-Free document understanding transformer. In *ECCV*, 2022.
- Alexander Kirillov, Eric Mintun, Nikhila Ravi, Hanzi Mao, Chloe Rolland, Laura Gustafson, Tete Xiao, Spencer Whitehead, Alexander C Berg, Wan-Yen Lo, et al. Segment anything. In *ICCV*, 2023.
- Byung-Kwan Lee, Beomchan Park, Chae Won Kim, and Yong Man Ro. MoAI: Mixture of all intelligence for large language and vision models. *arXiv:2403.07508*, 2024.
- Kenton Lee, Mandar Joshi, Iulia Raluca Turc, Hexiang Hu, Fangyu Liu, Julian Martin Eisenschlos, Urvashi Khandelwal, Peter Shaw, Ming-Wei Chang, and Kristina Toutanova. Pix2Struct: Screenshot parsing as pretraining for visual language understanding. In *ICML*, 2023.
- Bo Li, Yuanhan Zhang, Liangyu Chen, Jinghao Wang, Fanyi Pu, Jingkang Yang, Chunyuan Li, and Ziwei Liu. MIMIC-IT: Multi-modal in-context instruction tuning. *arXiv:2306.05425*, 2023a.
- Bo Li, Yuanhan Zhang, Liangyu Chen, Jinghao Wang, Jingkang Yang, and Ziwei Liu. Otter: A multi-modal model with in-context instruction tuning. *arXiv:2305.03726*, 2023b.
- Bohao Li, Rui Wang, Guangzhi Wang, Yuying Ge, Yixiao Ge, and Ying Shan. Seed-Bench: Benchmarking multimodal llms with generative comprehension. *arXiv:2307.16125*, 2023c.
- Chunyuan Li, Zhe Gan, Zhengyuan Yang, Jianwei Yang, Linjie Li, Lijuan Wang, Jianfeng Gao, et al. Multimodal foundation models: From specialists to general-purpose assistants. *Foundations and Trends® in Computer Graphics and Vision*, 2024a.
- Junnan Li, Dongxu Li, Caiming Xiong, and Steven Hoi. BLIP: Bootstrapping language-image pre-training for unified vision-language understanding and generation. In *ICML*, 2022.
- Junnan Li, Dongxu Li, Silvio Savarese, and Steven Hoi. BLIP-2: Bootstrapping language-image pre-training with frozen image encoders and large language models. In *ICML*, 2023d.

- Yanwei Li, Yuechen Zhang, Chengyao Wang, Zhisheng Zhong, Yixin Chen, Ruihang Chu, Shaoteng Liu, and Jiaya Jia. Mini-Gemini: Mining the potential of multi-modality vision language models. *arXiv:2403.18814*, 2024b.
- Yifan Li, Yifan Du, Kun Zhou, Jinpeng Wang, Wayne Xin Zhao, and Ji-Rong Wen. Evaluating object hallucination in large vision-language models. *arXiv:2305.10355*, 2023e.
- Zhang Li, Biao Yang, Qiang Liu, Zhiyin Ma, Shuo Zhang, Jingxu Yang, Yabo Sun, Yuliang Liu, and Xiang Bai. Monkey: Image resolution and text label are important things for large multi-modal models. In *CVPR*, 2024c.
- Ji Lin, Hongxu Yin, Wei Ping, Yao Lu, Pavlo Molchanov, Andrew Tao, Huizi Mao, Jan Kautz, Mohammad Shoeybi, and Song Han. VILA: On pre-training for visual language models. *arXiv:2312.07533*, 2023a.
- Ziyi Lin, Chris Liu, Renrui Zhang, Peng Gao, Longtian Qiu, Han Xiao, Han Qiu, Chen Lin, Wenqi Shao, Keqin Chen, et al. SPHINX: The joint mixing of weights, tasks, and visual embeddings for multi-modal large language models. *arXiv:2311.07575*, 2023b.
- Fuxiao Liu, Tianrui Guan, Zongxia Li, Lichang Chen, Yaser Yacoob, Dinesh Manocha, and Tianyi Zhou. HallusionBench: You see what you think? or you think what you see? an image-context reasoning benchmark challenging for gpt-4v (ision), llava-1.5, and other multi-modality models. *arXiv:2310.14566*, 2023a.
- Fuxiao Liu, Kevin Lin, Linjie Li, Jianfeng Wang, Yaser Yacoob, and Lijuan Wang. Aligning large multi-modal model with robust instruction tuning. *arXiv:2306.14565*, 2023b.
- Haotian Liu, Chunyuan Li, Yuheng Li, and Yong Jae Lee. Improved baselines with visual instruction tuning. *arXiv:2310.03744*, 2023c.
- Haotian Liu, Chunyuan Li, Qingyang Wu, and Yong Jae Lee. Visual instruction tuning. In *NeurIPS*, 2023d.
- Haotian Liu, Chunyuan Li, Yuheng Li, Bo Li, Yuanhan Zhang, Sheng Shen, and Yong Jae Lee. LLaVA-NeXT: Improved reasoning, ocr, and world knowledge. <https://llava-vl.github.io/blog/2024-01-30-llava-next/>, January 2024a.
- Shikun Liu, Linxi Fan, Edward Johns, Zhiding Yu, Chaowei Xiao, and Anima Anandkumar. Prism: A vision-language model with an ensemble of experts. *TMLR*, 2024b.
- Yuan Liu, Haodong Duan, Yuanhan Zhang, Bo Li, Songyang Zhang, Wangbo Zhao, Yike Yuan, Jiaqi Wang, Conghui He, Ziwei Liu, Kai Chen, and Dahua Lin. MMBench: Is your multi-modal model an all-around player? *arXiv:2307.06281*, 2023e.
- Yuliang Liu, Zhang Li, Biao Yang, Chunyuan Li, Xucheng Yin, Cheng lin Liu, Lianwen Jin, and Xiang Bai. On the hidden mystery of ocr in large multimodal models. *arXiv:2305.07895*, 2023f.
- Zhuang Liu, Hanzi Mao, Chao-Yuan Wu, Christoph Feichtenhofer, Trevor Darrell, and Saining Xie. A convnet for the 2020s. In *CVPR*, 2022.
- Pan Lu, Hritik Bansal, Tony Xia, Jiacheng Liu, Chunyuan Li, Hannaneh Hajishirzi, Hao Cheng, Kai-Wei Chang, Michel Galley, and Jianfeng Gao. MathVista: Evaluating mathematical reasoning of foundation models in visual contexts. In *ICLR*, 2024.
- Gen Luo, Yiyi Zhou, Yuxin Zhang, Xiawu Zheng, Xiaoshuai Sun, and Rongrong Ji. Feast your eyes: Mixture-of-resolution adaptation for multimodal large language models. *arXiv:2403.03003*, 2024.
- Ahmed Masry, Do Xuan Long, Jia Qing Tan, Shafiq Joty, and Enamul Hoque. ChartQA: A benchmark for question answering about charts with visual and logical reasoning. *arXiv:2203.10244*, 2022.
- Minesh Mathew, Dimosthenis Karatzas, and C. V. Jawahar. DocVQA: A dataset for vqa on document images. In *WACV*, 2021.

- Maxime Oquab, Timothée Darcet, Théo Moutakanni, Huy Vo, Marc Szafraniec, Vasil Khalidov, Pierre Fernandez, Daniel Haziza, Francisco Massa, Alaaeldin El-Nouby, et al. DINOv2: Learning robust visual features without supervision. *arXiv:2304.07193*, 2023.
- Alec Radford, Jong Wook Kim, Chris Hallacy, Aditya Ramesh, Gabriel Goh, Sandhini Agarwal, Girish Sastry, Amanda Askell, Pamela Mishkin, Jack Clark, et al. Learning transferable visual models from natural language supervision. In *ICML*, 2021.
- Mike Ranzinger, Greg Heinrich, Jan Kautz, and Pavlo Molchanov. AM-RADIO: Agglomerative vision foundation model reduce all domains into one. In *CVPR*, 2024.
- Tanik Saikh, Tirthankar Ghosal, Amish Mittal, Asif Ekbal, and Pushpak Bhattacharyya. ScienceQA: A novel resource for question answering on scholarly articles. *International Journal on Digital Libraries*, 2022.
- Christoph Schuhmann, Romain Beaumont, Richard Vencu, Cade W Gordon, Ross Wightman, Mehdi Cherti, Theo Coombes, Aarush Katta, Clayton Mullis, Mitchell Wortsman, Patrick Schramowski, Srivatsa R Kundurthy, Katherine Crowson, Ludwig Schmidt, Robert Kaczmarczyk, and Jenia Jitsev. LAION-5B: An open large-scale dataset for training next generation image-text models. In *NeurIPS Datasets and Benchmarks Track*, 2022. URL <https://openreview.net/forum?id=M3Y74vmsMcY>.
- Baifeng Shi, Ziyang Wu, Maolin Mao, Xin Wang, and Trevor Darrell. When do we not need larger vision models? *arXiv:2403.13043*, 2024.
- Wenzhe Shi, Jose Caballero, Ferenc Huszar, Johannes Totz, Andrew P. Aitken, Rob Bishop, Daniel Rueckert, and Zehan Wang. Real-time single image and video super-resolution using an efficient sub-pixel convolutional neural network. In *CVPR*, 2016.
- Amanpreet Singh, Vivek Natarajan, Meet Shah, Yu Jiang, Xinlei Chen, Dhruv Batra, Devi Parikh, and Marcus Rohrbach. Towards VQA models that can read. In *CVPR*, 2019.
- Quan Sun, Yuxin Fang, Ledell Wu, Xinlong Wang, and Yue Cao. EVA-CLIP: Improved training techniques for clip at scale. *arXiv:2303.15389*, 2023.
- Gemini Team, Rohan Anil, Sebastian Borgeaud, Yonghui Wu, Jean-Baptiste Alayrac, Jiahui Yu, Radu Soricut, Johan Schalkwyk, Andrew M Dai, Anja Hauth, et al. Gemini: a family of highly capable multimodal models. *arXiv:2312.11805*, 2023.
- Teknium. OpenHermes 2.5: An open dataset of synthetic data for generalist LLM assistants. <https://huggingface.co/datasets/teknium/OpenHermes-2.5>, 2023.
- Shengbang Tong, Ellis Brown, Penghao Wu, Sanghyun Woo, Manoj Middepogu, Sai Charitha Akula, Jihan Yang, Shusheng Yang, Adithya Iyer, Xichen Pan, Austin Wang, Rob Fergus, Yann LeCun, and Saining Xie. Cambrian-1: A fully open, vision-centric exploration of multimodal llms. *arXiv:2406.16860*, 2024.
- Junke Wang, Lingchen Meng, Zejjia Weng, Bo He, Zuxuan Wu, and Yu-Gang Jiang. To see is to believe: Prompting gpt-4v for better visual instruction tuning. *arXiv:2311.07574*, 2023a.
- Wei Han Wang, Qingsong Lv, Wenmeng Yu, Wenyi Hong, Ji Qi, Yan Wang, Junhui Ji, Zhuoyi Yang, Lei Zhao, Xixuan Song, et al. CogVLM: Visual expert for pretrained language models. *arXiv:2311.03079*, 2023b.
- Xiyang Wu, Ruiqi Xian, Tianrui Guan, Jing Liang, Souradip Chakraborty, Fuxiao Liu, Brian Sadler, Dinesh Manocha, and Amrit Singh Bedi. On the safety concerns of deploying llms/vlms in robotics: Highlighting the risks and vulnerabilities. *arXiv:2402.10340*, 2024.
- xAI. Grok-1.5 Vision Preview. <https://x.ai/blog/grok-1.5v>, 2024.
- xAI. Grok-1.5v. <https://x.ai/blog/grok-1.5v>, 2024. Accessed: 2024-09-28.
- Ruyi Xu, Yuan Yao, Zonghao Guo, Junbo Cui, Zanlin Ni, Chunjiang Ge, Tat-Seng Chua, Zhiyuan Liu, and Gao Huang. LLaVA-UHD: an lmm perceiving any aspect ratio and high-resolution images. *arXiv:2403.11703*, 2024.

- Shukang Yin, Chaoyou Fu, Sirui Zhao, Ke Li, Xing Sun, Tong Xu, and Enhong Chen. A survey on multimodal large language models. *IEEE Trans. PAMI*, 2024.
- Xiang Yue, Yuansheng Ni, Kai Zhang, Tianyu Zheng, Ruoqi Liu, Ge Zhang, Samuel Stevens, Dongfu Jiang, Weiming Ren, Yuxuan Sun, et al. MMMU: A massive multi-discipline multimodal understanding and reasoning benchmark for expert AGI. In *CVPR*, 2024.
- Yan Zeng, Hanbo Zhang, Jiani Zheng, Jiangnan Xia, Guoqiang Wei, Yang Wei, Yuchen Zhang, and Tao Kong. What matters in training a gpt4-style language model with multimodal inputs? *arXiv:2307.02469*, 2023.
- Xiaohua Zhai, Basil Mustafa, Alexander Kolesnikov, and Lucas Beyer. Sigmoid loss for language image pre-training. In *ICCV*, 2023.
- Yanzhe Zhang, Ruiyi Zhang, Jiuxiang Gu, Yufan Zhou, Nedim Lipka, Diyi Yang, and Tong Sun. LLaVAR: Enhanced visual instruction tuning for text-rich image understanding. *arXiv:2306.17107*, 2023.
- Deyao Zhu, Jun Chen, Xiaoqian Shen, Xiang Li, and Mohamed Elhoseiny. MiniGPT-4: Enhancing vision-language understanding with advanced large language models. *arXiv:2304.10592*, 2023.
- Xizhou Zhu, Weijie Su, Lewei Lu, Bin Li, Xiaogang Wang, and Jifeng Dai. Deformable DETR: Deformable transformers for end-to-end object detection. In *ICLR*, 2021.
- Yuke Zhu, Oliver Groth, Michael Bernstein, and Li Fei-Fei. Visual7W: Grounded Question Answering in Images. In *CVPR*, 2016.
- Zhuofan Zong, Bingqi Ma, Dazhong Shen, Guanglu Song, Hao Shao, Dongzhi Jiang, Hongsheng Li, and Yu Liu. MoVA: Adapting mixture of vision experts to multimodal context. *arXiv:2404.13046*, 2024.

A APPENDIX

A.1 BENCHMARK DETAILS

In this section, we provide the additional benchmark details for the tables in Section 2. The detailed comparison of different adaptation methods for the CLIP encoder are shown in Table 9. Table 10 shows the comparison between different vision encoders on all the adopted benchmarks. Table 11 list the detailed results on the vision encoder fusion methods. Table 12 shows the comparison between different vision encoder combinations on each benchmark.

Table 9: **Comparison of different high-resolution adaption methods to strengthen CLIP model (336x336)**. RWQA denotes the RealworldQA (xAI, 2024).

| Vision Encoder | Unfreeze | Res | GQA | VizWiz | MME | SEED | OCR | DocVQA | ChartQA | AI2D | POPE | RWQA | SQA | Avg. |
|--------------------|----------|-----|------|--------|------|------|-----|--------|---------|------|------|------|------|-------|
| <i>Original</i> | ✗ | 336 | 63.2 | 55.1 | 1574 | 70.2 | 354 | 59.6 | 42.1 | 71.1 | 86.7 | 58.0 | 72.5 | 616.5 |
| <i>Original</i> | ✓ | 336 | 60.9 | 54.0 | 1501 | 61.8 | 305 | 56.4 | 24.5 | 69.3 | 80.9 | 53.6 | 72.0 | 562.6 |
| <i>Interpolate</i> | ✗ | 448 | 62.7 | 53.8 | 1470 | 69.1 | 299 | 58.4 | 37.7 | 71.2 | 85.7 | 55.3 | 69.6 | 589.7 |
| <i>Interpolate</i> | ✓ | 448 | 65.6 | 57.8 | 1534 | 73.7 | 526 | 65.0 | 61.1 | 73.7 | 87.3 | 57.7 | 71.5 | 670.5 |
| <i>Interpolate</i> | ✓ | 672 | 64.9 | 55.7 | 1503 | 72.4 | 509 | 64.6 | 62.0 | 72.2 | 87.1 | 57.4 | 71.2 | 674.2 |
| <i>Tiled-input</i> | ✓ | 672 | 63.0 | 54.9 | 1529 | 72.5 | 435 | 64.9 | 65.7 | 71.5 | 87.6 | 57.0 | 71.4 | 673.9 |
| <i>InternVL</i> | ✗ | 448 | 63.6 | 56.9 | 1537 | 71.7 | 529 | 65.0 | 58.6 | 72.9 | 87.4 | 59.2 | 70.2 | 661.9 |
| <i>InternVL</i> | ✓ | 448 | 65.6 | 57.8 | 1534 | 73.7 | 526 | 65.0 | 61.1 | 73.7 | 87.3 | 58.8 | 71.5 | 671.5 |

Table 10: **Comparison between different vision experts as the MLLM encoders.**

| Category | Vision Encoder | Unfreeze | Res | GQA | VizWiz | MME | SEED | OCR | DocVQA | ChartQA | AI2D | POPE | RWQA | SQA | Avg. |
|-------------------------|-------------------|----------|------|------|--------|------|------|-----|--------|---------|------|------|------|------|-------|
| <i>VL Alignment</i> | <i>ConvNeXt</i> | ✗ | 1024 | 63.3 | 53.5 | 1526 | 70.6 | 404 | 70.4 | 60.8 | 71.6 | 87.5 | 57.1 | 68.6 | 635.0 |
| | | ✓ | 1024 | 63.3 | 54.4 | 1510 | 72.9 | 518 | 77.9 | 67.0 | 72.1 | 88.1 | 58.8 | 68.6 | 659.7 |
| <i>Segmentation</i> | <i>SAM</i> | ✗ | 1024 | 57.3 | 49.0 | 1216 | 56.9 | 38 | 20.1 | 17.4 | 69.2 | 84.3 | 49.2 | 66.8 | 471.1 |
| | | ✓ | 1024 | 60.2 | 51.5 | 1291 | 65.9 | 35 | 21.2 | 17.8 | 70.7 | 86.4 | 54.1 | 65.7 | 494.7 |
| <i>Object Detection</i> | <i>EVA-02</i> | ✗ | 1024 | 63.1 | 51.1 | 1359 | 69.2 | 123 | 25.6 | 25.2 | 71.2 | 88.5 | 57.9 | 66.1 | 523.5 |
| | | ✓ | 1024 | 64.3 | 55.5 | 1449 | 72.7 | 358 | 57.1 | 57.5 | 72.2 | 88.3 | 59.6 | 67.7 | 614.4 |
| <i>Text Recognition</i> | <i>Pix2Struct</i> | ✗ | 1024 | 53.1 | 48.1 | 1296 | 53.4 | 460 | 71.0 | 61.0 | 69.6 | 79.2 | 46.7 | 65.5 | 578.7 |
| | | ✓ | 1024 | 54.9 | 47.3 | 1262 | 55.1 | 472 | 72.5 | 62.0 | 68.7 | 80.0 | 49.3 | 66.6 | 584.8 |
| <i>Self-Supervised</i> | <i>DINOv2</i> | ✗ | 448 | 62.4 | 53.1 | 1438 | 67.4 | 41 | 20.2 | 17.3 | 70.7 | 85.3 | 53.3 | 67.1 | 503.1 |
| | | ✓ | 448 | 64.2 | 55.5 | 1466 | 71.8 | 45 | 20.4 | 17.5 | 71.4 | 87.4 | 57.3 | 67.8 | 518.0 |

Table 11: **Comparison of different fusion methods for different vision experts.** “#Tokens(V)” denotes the number of visual tokens.

| Vision Encoders | Fusion | #Tokens(V) | GQA | VizWiz | MME | SEED | OCR | DocVQA | ChartQA | AI2D | POPE | RWQA | SQA | Avg. |
|------------------------------|-------------------------|------------|------|--------|------|------|-----|--------|---------|------|------|------|------|-------|
| <i>CLIP + ConvNeXt</i> | <i>Seq. Append</i> | 2048 | 64.8 | 54.5 | 1563 | 73.4 | 532 | 77.7 | 67.6 | 72.4 | 87.9 | 61.2 | 68.8 | 690.5 |
| | <i>Channel Concat.</i> | 1024 | 63.2 | 48.0 | 1497 | 73.5 | 551 | 77.7 | 67.0 | 72.4 | 88.3 | 59.1 | 70.7 | 681.5 |
| | <i>LLaVA-HR</i> | 1024 | 64.5 | 57.2 | 1538 | 72.0 | 498 | 74.5 | 63.8 | 72.3 | 87.7 | 59.2 | 68.7 | 678.7 |
| | <i>Mini-Gemini</i> | 1024 | 65.3 | 56.9 | 1548 | 72.9 | 478 | 68.3 | 63.2 | 71.5 | 87.3 | 59.7 | 69.4 | 672.5 |
| | <i>Deformable Attn.</i> | 1024 | 64.0 | 57.3 | 1504 | 72.7 | 463 | 69.5 | 64.4 | 73.3 | 87.4 | 62.8 | 68.9 | 674.3 |
| <i>CLIP + ConvNeXt + SAM</i> | <i>Seq. Append</i> | 3072 | 64.3 | 53.6 | 1539 | 73.2 | 525 | 77.9 | 67.0 | 72.3 | 87.4 | 60.1 | 69.5 | 686.2 |
| | <i>Channel Concat.</i> | 1024 | 63.3 | 55.9 | 1528 | 73.3 | 545 | 78.9 | 67.2 | 72.3 | 88.4 | 59.2 | 70.0 | 690.4 |

Table 12: Detailed comparison on vision encoder combinations.

| #Encoder | Encoder Combination | GQA | VizWiz | MME | SEED | OCR | DocVQA | ChartQA | AI2D | POPE | RWQA | SQA | Avg. |
|----------|-----------------------------|------|--------|--------|------|-------|--------|---------|------|------|------|------|-------|
| 2 | CL + CN | 63.2 | 48.0 | 1497.0 | 73.5 | 551.0 | 77.7 | 67.0 | 72.4 | 88.3 | 59.1 | 70.7 | 681.5 |
| 3 | CL + CN + DI | 63.3 | 55.9 | 1528.0 | 73.3 | 545.0 | 78.9 | 67.2 | 72.3 | 88.4 | 59.2 | 70.0 | 690.4 |
| | CL + CN + SA | 64.6 | 55.3 | 1504.0 | 73.3 | 526.0 | 75.7 | 64.9 | 72.1 | 88.3 | 61.1 | 70.9 | 685.4 |
| | CL + CN + PS | 63.2 | 51.4 | 1497.0 | 73.3 | 550.0 | 78.5 | 65.9 | 73.1 | 87.7 | 60.3 | 70.5 | 685.1 |
| | CL + CN + EV | 63.2 | 51.7 | 1565.0 | 73.9 | 538.0 | 77.7 | 67.8 | 73.6 | 89.0 | 61.4 | 69.4 | 690.7 |
| | CL + CN + EV + DI | 63.6 | 54.9 | 1512.0 | 73.8 | 547.0 | 77.0 | 66.7 | 73.1 | 88.9 | 60.4 | 69.7 | 689.4 |
| | CL + CN + EV + SA | 64.3 | 57.7 | 1533.0 | 73.7 | 521.0 | 75.2 | 65.3 | 72.2 | 88.5 | 61.1 | 70.2 | 688.0 |
| | CL + CN + EV + PS | 64.8 | 56.5 | 1561.0 | 73.4 | 540.0 | 78.8 | 67.5 | 72.2 | 88.4 | 59.9 | 70.5 | 694.6 |
| 5 | CL + CN + EV + PS + SA | 64.7 | 59.1 | 1528.0 | 73.9 | 529.0 | 78.6 | 67.8 | 72.9 | 88.8 | 62.2 | 69.7 | 697.1 |
| | CL + CN + EV + PS + DI | 64.7 | 54.1 | 1506.0 | 73.7 | 541.0 | 75.1 | 64.9 | 72.7 | 88.3 | 60.0 | 70.3 | 684.7 |
| 6 | CL + CN + EV + PS + SA + DI | 63.8 | 57.8 | 1512.0 | 73.5 | 525.0 | 75.1 | 65.8 | 71.8 | 88.4 | 61.4 | 69.9 | 686.8 |

Table 13: Comparison between different training strategies. ‘1 epoch’ means we train *Eagle* for 1 epoch in the supervised fine-tuning stage. ‘unlock*’ means we unlock vision encoders in the pre-training stage.

| Config | Prealign | Pretrain | Finetune | GQA | MME | OCR | SciQA | POPE | DocVQA | ChartQA | SEED | Vizwiz | AI2D | RWQA | Avg. |
|------------------|---------------------|---------------------|-----------|------|------|------|-------|------|--------|---------|------|--------|------|------|--------------|
| 1 epoch | ✗ | llava595k | Eagle1.8M | 64.7 | 1528 | 52.9 | 69.7 | 88.8 | 78.6 | 67.7 | 73.9 | 59.1 | 72.8 | 62.2 | 697.1 |
| 2 epoch | ✗ | llava595k | Eagle1.8M | 65.4 | 1539 | 51.4 | 70.3 | 87.9 | 79.8 | 67.9 | 73.8 | 58.5 | 73.5 | 62.7 | 698.3 |
| 1 epoch, unlock* | ✗ | llava595k | Eagle1.8M | 64.1 | 1541 | 54.4 | 71.5 | 88.5 | 79.1 | 68.5 | 74.0 | 56.6 | 72.2 | 61.9 | 698.0 |
| 1 epoch, unlock* | ✗ | llava595k+Eagle1.8M | Eagle1.8M | 65.3 | 1545 | 54.8 | 70.5 | 88.5 | 78.8 | 68.4 | 73.5 | 57.5 | 72.0 | 62.9 | 699.5 |
| 1 epoch | Eagle1.8M | llava595k | Eagle1.8M | 64.5 | 1579 | 55.4 | 71.6 | 88.7 | 79.3 | 68.9 | 73.9 | 58.9 | 73.9 | 63.4 | 706.6 |
| 1 epoch, unlock* | Eagle1.8M | llava595k | Eagle1.8M | 65.1 | 1561 | 56.0 | 71.3 | 88.5 | 79.3 | 69.5 | 74.2 | 59 | 73.5 | 63.4 | 707.1 |
| 1 epoch, unlock* | llava595k+Eagle1.8M | llava595k | Eagle1.8M | 64.5 | 1570 | 56.0 | 71.7 | 89 | 79.7 | 68.9 | 74.0 | 58.5 | 74.0 | 63.7 | 707.8 |
| 1 epoch, unlock* | llava595k+Eagle1.8M | llava595k+Eagle1.8M | Eagle1.8M | 64.6 | 1582 | 56.6 | 71.9 | 88.7 | 79.8 | 69.3 | 73.7 | 58.7 | 73.5 | 63.9 | 708.9 |

A.2 ADDITIONAL QUALITATIVE RESULTS

Fig. 6 demonstrates that our model can perform reasoning based on the knowledge to answer some difficult questions. Fig. 7 shows some examples of OCR and document understanding cases.

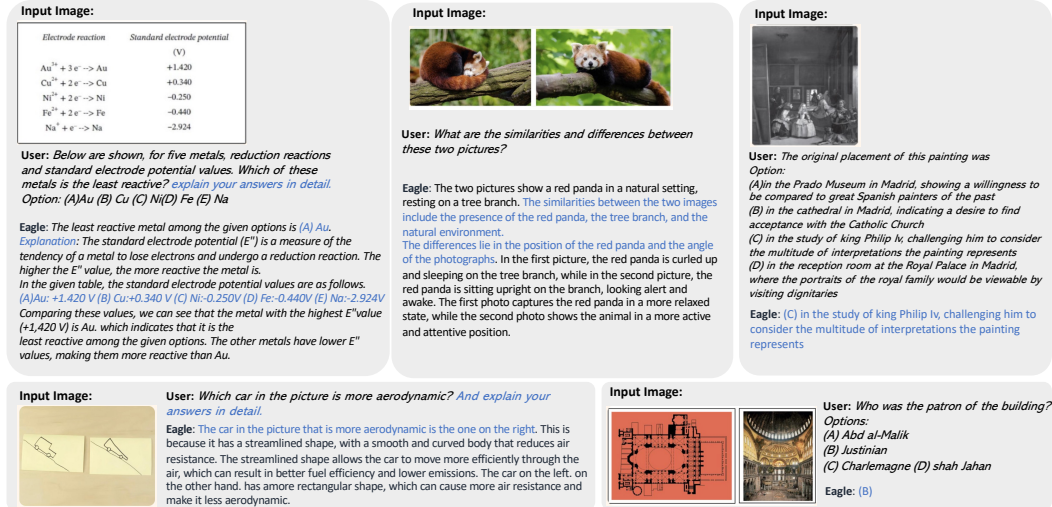


Figure 6: Qualitative results of Eagle on VQA tasks requiring college-level knowledge or deliberate reasoning.

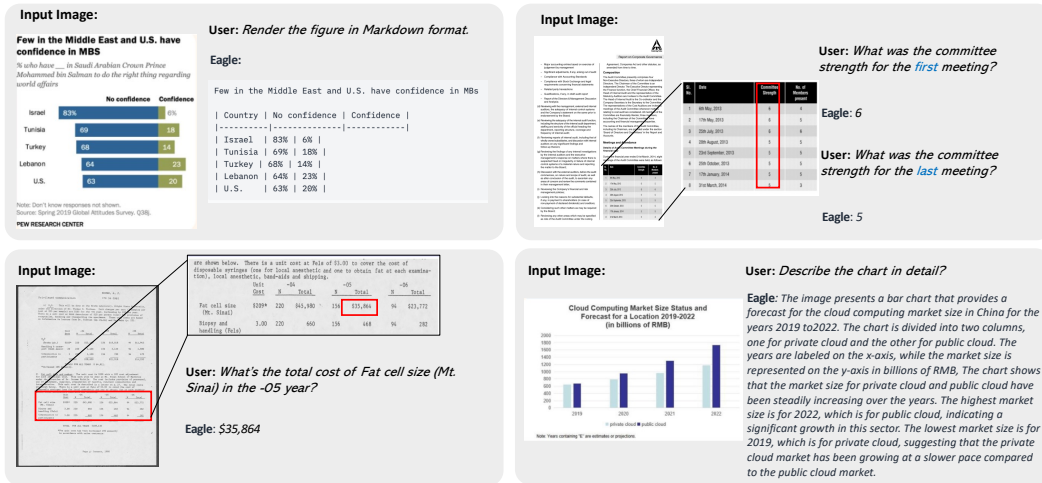


Figure 7: Qualitative samples on OCR and document understanding tasks. Eagle is able to extract useful information from small text.